Quasiclassical Kinetics of the $H_2 + H_2$ Reaction and Dissociation

A. Ceballos

Departamento de Quimica Fisica, Universidad de Salamanca, 37008 Salamanca, Spain

E. Garcia and A. Rodriguez

Departamento de Quimica Fisica, Universidad del Pais Vasco, 01006 Vitoria, Spain

A. Laganà*

Dipartimento di Chimica, Università di Perugia, 06123 Perugia, Italy

Received: July 31, 2000; In Final Form: December 12, 2000

We have investigated the elementary processes occurring in $H_2 + H_2$ collisions by integrating large batches of quasiclassical trajectories. This has allowed us to calculate the vibrational state-selected rate coefficients as well as their aggregations in classes leading to the same products and their dependence on temperature. The contribution of the various elementary and aggregated processes both to the allocation of energy among the various vibrational states of the products and to the production of hydrogen atoms is analyzed. Some correlations of these contributions with the value of the impact parameter and with some characteristics of the reactive mechanism are also discussed. The key importance of hydrogen exchange processes is also singled out.

Introduction

Recently, the interest for studying four and more atom collision processes has considerably increased.[1] The objective of such a study is not only to enhance our understanding of the mechanisms governing many center collisions but also to provide realistic model treatments for systems of practical relevance using a priori estimates of rate coefficients.

This is, indeed, the case of the $H_2 + H_2$ collision processes. From the theoretical point of view, these processes are important because they couple an exchange reaction with the fragmentation of the reactants into atoms while being still treatable using a priori dynamical methods. From the practical point of view, the knowledge of rate coefficients of the $H_2 + H_2$ processes is relevant to the modeling of nonequilibrium systems of interest for astrophysical,[2] combustion[3], and spacecraft[4] applications as well as for the production of light negative ions.[5] In all of these cases, a fundamental input information is the set of detailed $H_2 + H_2$ state-selected rate coefficients.

Experimental information on these rate coefficients is contained in refs 6 and 7. Nonlinear optical methods (CARS probing, stimulated Raman excitation, and photoacustic detection techniques[6−12]) are a valuable source of nonreactive V−V (vibration to vibration) and V−T/R (vibration to translation/rotation) energy-transfer rate coefficients.

On the theoretical side, despite the very light mass of H, a full dimensional quantum mechanical (QM) investigation of $H_2 + H_2$ processes is impractical at present because of the high barrier to reaction (the barrier energy is larger than the H_2 dissociation energy) characterizing the potential energy surface (PES) of this system.

The need for supplying a significant amount of energy before allowing the system to react implies that a large expansion basis set has to be used and that dissociation wave functions and boundary conditions (not to mention that the formalism of four center reactions, like the title one, is in itself quite complex) have to be included in the theoretical treatment.

Accordingly, up to now, only a reduced dimensionality (RD) quantum calculation has been performed[13] for $H_2 + H_2$. This QM RD dynamical treatment assumes that reactive encounters take place on a plane (with the four atoms being located at the corners of a trapezium) and that the internuclear axes of the colliding molecules (the two bases of the trapezium) approach with a zero-impact parameter. Using this model, quantum probabilities of collision-induced dissociation (CID) and a four-center exchange reaction (4C) were calculated at collision energies ranging from threshold to just above 125 kcal/mol. RD quasiclassical trajectory (QCT) results[14] agree with RD QM ones in indicating that internal energy (and in particular vibrational energy) plays a key role in promoting dissociation. For $H_2 + H_2$ collisions, semiclassical calculations were also performed.[15] However, because they were performed only for the lowest vibrational states, no indication was obtained on the role played by vibrational energy in promoting reaction and dissociation.

Full-dimensional QCT calculations are much easier to carry out. Despite this, only limited full-dimensional quasiclassical calculations have been reported in the literature.[2,14,16] In ref 2, the thermal CID rate coefficients of $H_2 + H_2$ were evaluated considering one of the two hydrogen molecules in its ground state. In ref 16, the effect of the initial vibration, rotation and translation on the amount of collisional energy transferred during the process was evaluated at total energies of 62 and 157 kcal/mol and small values of the impact parameters. In our previous study,[14] full dimensional QCT calculations were performed in order to investigate the validity of the RD model and the mechanisms of the exchange and dissociative processes.

* To whom correspondence should be addressed.

10.1021/jp002727f CCC: $20.00
Published on Web 02/21/2001

For the studies of refs 2 and 16, the PES of ref 17 was used. For the QM and QCT RD calculations of refs 13 and 14, the PES of Paniagua et al[18] was used. Although the two PESs were derived from the same extended set of accurate (MRD-CI) electronic energies,[19] the PES of ref 18 has been described in more detail in the literature. Its root-mean-square deviation is 1.4 kcal/mol. Its transition state is linear, with the two inner H atoms being separated by 0.748 Å and the two outer atoms being separated by 4.141 Å. The transition state has an energy 111.1 kcal/mol higher than the asymptotic minimum of the reactants $H_2 + H_2$, i.e., it lies 1.6 kcal/mol above the H_2 dissociation limit.

Calculated Quantities

Details of the computational method used for the QCT calculation of rate coefficients are given elsewhere.[14,20] Here, only some complementary details needed to understand the work reported in the paper are discussed.

Elementary processes involved in $H_2 + H_2$ collisions are the following:

$$\text{(P0)}\ H_1H_2(v_{1-2},j_{1-2}) + H_3H_4(v_{3-4},j_{3-4}) \xrightarrow{n} H_1H_2(v'_{1-2},j'_{1-2}) + H_3H_4(v'_{3-4},j'_{3-4})$$

$$\text{(P1)}\ H_1H_2(v_{1-2},j_{1-2}) + H_3H_4(v_{3-4},j_{3-4}) \xrightarrow{r} H_1H_3(v'_{1-3},j'_{1-3}) + H_2H_4(v'_{2-4},j'_{2-4})$$

$$\text{(P2)}\ H_1H_2(v_{1-2},j_{1-2}) + H_3H_4(v_{3-4},j_{3-4}) \xrightarrow{r} H_1H_4(v'_{1-4},j'_{1-4}) + H_2H_3(v'_{2-3},j'_{2-3})$$

$$\text{(P3)}\ H_1H_2(v_{1-2},j_{1-2}) + H_3H_4(v_{3-4},j_{3-4}) \xrightarrow{n_d} H_1H_2(v'_{1-2},j'_{1-2}) + H_3(k'_3) + H_4(k'_4)$$

$$\text{(P4)}\ H_1H_2(v_{1-2},j_{1-2}) + H_3H_4(v_{3-4},j_{3-4}) \xrightarrow{r_d} H_1H_3(v'_{1-3},j'_{1-3}) + H_2(k'_2) + H_4(k'_4)$$

$$\text{(P5)}\ H_1H_2(v_{1-2},j_{1-2}) + H_3H_4(v_{3-4},j_{3-4}) \xrightarrow{r_d} H_1H_4(v'_{1-4},j'_{1-4}) + H_2(k'_2) + H_3(k'_3)$$

$$\text{(P6)}\ H_1H_2(v_{1-2},j_{1-2}) + H_3H_4(v_{3-4},j_{3-4}) \xrightarrow{r_d} H_2H_3(v'_{2-3},j'_{2-3}) + H_1(k'_1) + H_4(k'_4)$$

$$\text{(P7)}\ H_1H_2(v_{1-2},j_{1-2}) + H_3H_4(v_{3-4},j_{3-4}) \xrightarrow{r_d} H_2H_4(v'_{2-4},j'_{2-4}) + H_1(k'_1) + H_3(k'_3)$$

$$\text{(P8)}\ H_1H_2(v_{1-2},j_{1-2}) + H_3H_4(v_{3-4},j_{3-4}) \xrightarrow{n_d} H_3H_4(v'_{3-4},j'_{3-4}) + H_1(k'_1) + H_2(k'_2)$$

$$\text{(P9)}\ H_1H_2(v_{1-2},j_{1-2}) + H_3H_4(v_{3-4},j_{3-4}) \xrightarrow{d} H_1(k'_1) + H_2(k'_2) + H_3(k'_3) + H_4(k'_4)$$

where primed quantities are for products and unprimed ones for reactants. In the remainder of the paper, no explicit reference will be made to rotations because the considered quantities are, in general, Boltzmann averaged over initial rotation and translation (reactants are thermalized) and summed over final rotational states. In other words, quantities discussed here are the vibrational state-selected rates.

Process P0 is the nonreactive (elastic and inelastic) energy exchange *n*. The corresponding rates, however, refer to the pure inelastic component because elastic contributions are, as usual, not converged. Processes P1 and P2 are both reactive exchanges *r*. Processes P3 and P8 are both nonreactive dissociations n_d. Processes P4−P7 are the dissociative reactive exchanges r_d. Process P9 is full dissociation *d*. The vibrational states of the reactants are labeled as v_{1-2} and v_{3-4}, whereas the vibrational states of the products are labeled as v'_{1-2} and v'_{3-4} if the process is nonreactive elastic or inelastic and v'_{1-3}, v'_{1-4}, v'_{2-3}, and v'_{2-4} if the process is reactive. When the reactive process is accompanied by dissociative fragmentation, atomic products are characterized by the appropriate wavenumbers (k'_1, k'_2, k'_3, and k'_4) rather than by the internal energy quantum number.

As was already mentioned, for all of these processes we calculated vibrational state-selected rate coefficients. For a given process *P*, vibrational state-selected rate coefficients are formulated as

$$k_P(v_{1-2}, v_{3-4}, T) = \left(\frac{8k_BT}{\pi\mu}\right)^{1/2} \pi b_{max}^2 \frac{N^P_{v_{1-2},v_{3-4}}}{N_{v_{1-2},v_{3-4}}} \qquad (1)$$

where $N_{v_{1-2},v_{3-4}}$ is the number of trajectories integrated starting from the v_{1-2} and v_{3-4} pair of initial vibrational states at the translational and rotational temperature *T*. In the same equation, $N^P_{v_{1-2},v_{3-4}}/N_{v_{1-2},v_{3-4}}$ is the fraction of $N_{v_{1-2},v_{3-4}}$ following process *P*, k_B is the Boltzmann constant, and μ is the reduced mass of the two colliding diatomic molecules.

The present investigation focuses upon the effect of varying the initial conditions of the colliding hydrogen molecules on the value of the rate coefficient for the different types of processes. It focuses also upon the vibrational distribution of the products, i.e., the allocation of energy in the vibrational modes of the products (discrete quantum numbers for the products have been obtained by rounding the quasiclassical vibrational number to the nearest integer) by aggregating together events leading to the same type of products. To rationalize the behavior of the system, we also analyze some auxiliary quantities like the state-selected opacity function.

QCT calculations were run for values of the initial vibrational energy of the reactants corresponding to all of the 15 possible combinations of the vibrational quantum numbers 5, 7, 9, 11, and 13. The translational and rotational energies were selected according to the Boltzmann distribution for $T = T_{rot} = T_{tr} =$ 1000, 2000, and 4000 K. An integration step of 0.15 fs was used to guarantee a good total energy and angular momentum conservation. For each set of initial conditions, a batch of 100 000 trajectories was run using a maximum impact parameter b_{max} equal to 4.0 Å. When necessary, to converge results at a larger b_{max}, additional trajectories were integrated by increasing the value of the maximum impact parameter in steps of 0.2 Å. For the highest vibrational states, it was necessary to increase the value of b_{max} up to 5.8 Å before obtaining a contribution smaller than 1% in the highest bin. Larger batches of trajectories were integrated also when, mainly at low vibrational states and temperatures, the number of trajectories contributing to the quantity being calculated was small. Accordingly, the number of calculated trajectories ranges from 110 250 (for $v_{1-2} = v_{3-4} = 9$ and $T = 4000$ K) to 600 000 (for $v_{1-2} = v_{3-4} = 5$ and $T = 1000$ K). This makes the overall number of integrated trajectories larger than 10 000 000. The error estimated for the calculated state-selected rates was smaller than 2% with the exception of those at low vibrational states and temperatures.

To determine the internal states of the products, the trajectories are stopped when at least four of the six internuclear distances exceed the value of 8 Å and the internal (kinetic and potential) energy of each pair of atoms is calculated. A pair of atoms are considered as bound when their internal energy is smaller than the dissociation limit. On this ground, one can figure out what process is taking place. Related rotational and vibrational quantum numbers are determined by applying the usual discretization recipe:[21] (1) the rotational angular momentum and the rotational number are calculated; (2) the vibrational number are calculated using a semiclassical method; and (3) the continuous rotational and vibrational numbers are rounded to the nearest integer.

More complex is the calculation of nonreactive properties (as is well-known, elastic QCT rate coefficients do not converge with the impact parameter). Here, we take as elastic the collisions for which both the H_1H_2 and the H_3H_4 final vibrational numbers coincide with the initial ones ($v'_{1-2} = v_{1-2}$ and $v'_{3-4} = v_{3-4}$). However, there are processes for which the separation between elastic and nonelastic processes is more subtle. As an example, dissociation can occur also for nonreactive collisions. In this case, at the highest vibrational state considered in the present calculation ($v_{1-2} = 13$), when the rotational number is as high as $j_{1-2} = 7$, the internal energy is only 0.12 kcal/mol smaller than the dissociation limit. As a consequence, the molecules are very close to dissociation, and such a process may take place also at long range. This makes the convergence of the calculated rate coefficients so slow that it can be masked by the fluctuations because of the statistical sampling. For this reason, at $v_{1-2} = 13$, we consider as elastic all of the collisions leading to a final H_1H_2 molecule with a vibrational number $v'_{1-2} = 13$ and not having an internal energy higher than 0.13 kcal/mol above the dissociation limit (0.13 kcal/mol is half of the energy of the first quasibound state for H_2 ($v = 13$, $j = 8$)).

Rate Coefficients

State-selected aggregated rates for inelastic, reactive, nonreactive dissociative, reactive dissociative, and full-dissociative processes are plotted in Figure 1 as a function of the temperature *T*. Each panel contains these rate coefficients for a given pair of vibrational states. The figure is symmetric because of the symmetry of the system.

An inspection of the figure shows that in several cases the dissociative reaction is the dominant process. This is not the case, however, when the content of the vibrational energy of the collision partners is low. In these cases, inelastic processes are dominant. This happens also when a reactant molecule is highly excited while the other has low or no vibrational excitation (as an example when $v_{1-2} = 13$ and $v_{3-4} = 5$). In these cases, the nonreactive process is accompanied by dissociation. Reactive dissociation (the dissociation occurring after or while an exchange of the molecular partners is taking place) implies that both initial H_2 bonds break to generate a new bond. In the range of temperatures considered here, we find that this process is the most efficient when one of the reactant molecules is close to dissociation (e.g., $v = 13$) and the sum of the vibrational numbers of the two reactant molecules exceeds 20. In this situation, also nonreactive encounters lead preferentially to dissociation. Reactive-dissociation rate coefficients are usually twice as large as the nonreactive ones except for the highest vibrational states. Efficiency of full dissociation is always low with the exception of very high vibrational states and temperatures.

Of the four aggregated processes discussed in detail in this paper (full dissociation is not included because in most cases

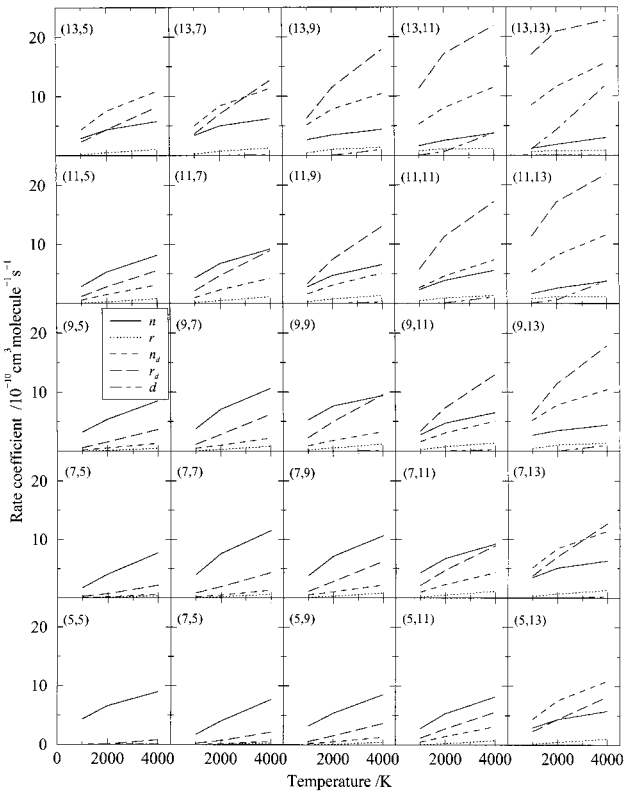

Figure 1. State-selected inelastic (solid line), reactive (dotted line), nonreactive dissociative (short-dashed line), reactive dissociative (long-dashed line) and full-dissociative (dashed−dotted line) rate coefficients calculated at given pairs of vibrational numbers (indicated in brackets) for rotationally and translationally thermalilzed reactants plotted as a function of the temperature.

the value of the related rate coefficients is so small that it cannot be appreciated in the plot scale) the least efficient one is the exchange of molecular partners without dissociation (plain reaction). This is true even when, at low vibrational excitation of the reactants, nonreactive dissociation has little chance to occur. Obviously, when the vibrational excitation of reactants is small, the most favorite processes are inelastic collisions. The high efficiency of inelastic collisions at low vibrational energy has been already investigated by Cacciatore and Billing.[15] They performed accurate semiclassical nonreactive calculations of rate coefficients for $H_2 + H_2$ collisions and compared calculated values with experimental results. Present calculations indicate, however, that the high vibrational energy regime is different.

As temperature increases, all processes become more efficient at the expenses of purely elastic ones. The efficiency increase for reactive, nonreactive dissociative and reactive dissociative rate coefficients depends on the nature of the process. Dissociative processes are significantly enhanced by an increase of the vibrational energy of reactants. Such an enhancement is more evident when reactant molecules (at least one of them) are already in a highly excited vibrational state. Also, dissociative processes increase markedly when temperature increases. Often, the reactive dissociation is more important than the nonreactive one and the difference becomes larger as both the initial vibrational state and the temperature increase. On the contrary, reactive rate coefficients undergo a moderate enhancement when initial vibrational energy and temperature increase.

A last comment is deserved by the inelastic rate coefficients (their estimates have to be considered with some caution because of the essentially arbitrary nature of the QCT recipes for discretizing classical states especially for small changes of

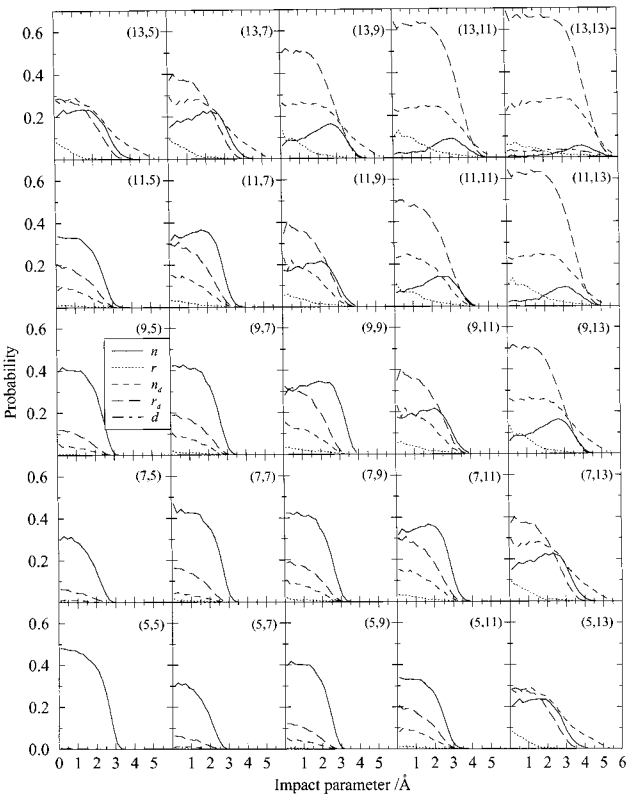

Figure 2. Inelastic (solid line), reactive (dotted line), nonreactive dissociative (short-dashed line), reactive dissociative (long-dashed line), and full-dissociative (dashed−dotted line) probabilities calculated at given pairs of vibrational numbers (indicated in brackets) plotted as a function of the impact parameter for rotationally and translationally thermalized reactants at $T = 1000$ K.

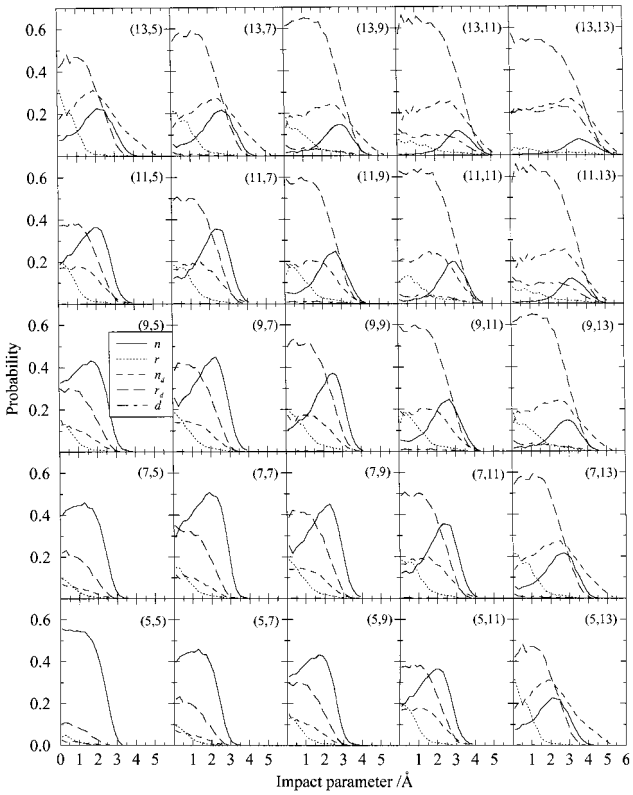

Figure 3. Inelastic (solid line), reactive (dotted line), nonreactive dissociative (short-dashed line), reactive dissociative (long-dashed line), and full dissociative (dashed−dotted line) probabilities calculated at given pairs of vibrational numbers (indicated in brackets) plotted as a function of the impact parameter for rotationally and translationally thermalized reactants at $T = 4000$ K.

vibrational energy and for energies close to dissociation). As is shown in Figure 1, inelastic rate coefficients increase more when the temperature rises from 1000 to 2000 K than in the interval 2000−4000 K. The figure shows also that at high reactant vibrational numbers inelastic rate coefficients are lower because of the increasing importance of dissociation processes.

A peculiar feature of the $H_2 + H_2$ collision processes is the role played by the exchange of the molecular partners even when the system dissociates. This is due to the combination of two important characteristics of the title system: symmetry and lightness. The fact that the hydrogen atom is highly mobile because of its lightness and that once it reaches with the appropriate velocity the proximity of another hydrogen means it is only a matter of semantic to say what pair of atoms is bound in a molecule while the four atoms are interacting. This makes the exchange of molecular partners quite likely in vibrationally excited molecules containing hydrogen atoms.

Opacity Functions

As was already mentioned, to understand the behavior of the $H_2 + H_2$ system we examine also other quantities which can shed some light on the nature of the investigated processes. The first quantity we consider (see Figures 2 and 3) is the opacity function, i.e., the variation of the probability with the impact parameter, calculated at $T = 1000$ and 4000 K, respectively. The opacity function was determined using a histogrammic method that segments the range of the impact parameter b in boxes of 0.2 Å.

The opacity function for inelastic processes shows a definite variation with the vibrational number and with the temperature. In Figure 2, values of the inelastic probability (summed over all final vibrational and rotational states) calculated at $T = 1000$ K are shown as solid lines. From the figure, one can easily see that the shape of the opacity function at $v_{1-2} = v_{3-4} = 5$ is the typical classical (hard sphere-like) one, having a plateau at about 0.45 for b ranging from 0 to 2 Å and sharply dropping afterward. When one of the vibrational numbers increases, the range of b values for which the probability is nonzero almost imperceptibly widens, whereas in general, the height of the plateau slightly lowers. This explains why, with the only exception of the $v_{1-2} = 5$ and $v_{3-4} = 7$ case (and vice versa) for which the lowering is particularly pronounced, the value of the inelastic rate coefficient monotonically decreases as vibrational excitation increases. This is confirmed by the fact that, when both initial vibrational numbers increase, the decrease of the value of the inelastic rate coefficient is even larger. In these cases, the shape of the opacity function changes and, instead of forming a plateau at low b values and then decreasing, it first increases with b up to a maximum (at approximately $b = 3$ Å) and then decreases. This erosion of the probability at small values of the impact parameter implies that these processes tend to be increasingly associated with less direct attacks. The transition between these two behaviors occurs at $v_{1-2} = v_{3-4} = 9$ for which the plateau extends to $b = 3$ Å, resulting in larger rate coefficients. An increase of the temperature enhances the role played by less direct attacks associated with large-impact parameter collisions by further eroding low b probabilities. As Figure 3 shows, the transition between the two behaviors occurs at about $v_{1-2} = v_{3-4} = 7$. However, to the end of determining the value of rate coefficients (the other factor is the greater average velocity as the temperature increases), the shrinking of the area covered

by the opacity function is, at least partially, compensated by the shift of its maximum to a higher value of *b*.

An opposite shape is obtained for the reactive (dissociationless) exchange processes (dotted lines in Figures 2 and 3). In this case, impact parameter values close to zero are the most effective in promoting these processes, whose efficiency decreases as the impact parameter increases. This is in line with the assumptions of the model treatment adopted in ref 13. An increase of the vibrational numbers (moving up and to the left of the figure) has the effect of increasing the value of the probability at the maximum and of widening the interval of accessible impact parameter values. A comparison of Figures 2 and 3 shows that a rise of the temperature increases the value of the probability at the maximum while the interval of accessible impact parameters is not affected. However, when the two initial molecules have a very large vibrational excitation, the probability that a reactive exchange occurs decreases as the temperature increases. This can be rationalized in terms of a dominance of dissociative processes. Nevertheless, such a decrease of the probability with the temperature is more than compensated by the corresponding increase of the average velocity, making the reactive rate coefficients increase with temperature.

A substantially similar behavior is found for dissociative processes (both nonreactive and reactive, plotted as short- and long-dashed lines, respectively, in Figures 2 and 3). The opacity function at low temperature and low vibrational excitation of the reactants has a small maximum at zero-impact parameter, and the probability decreases almost linearly as the impact parameter increases. However, when the vibrational energy of the reactants increases, a plateau (or a shallow maximum) gradually builds up in the plot and the accessible range of *b* values widens. For reactive processes, the formation of the plateau begins at lower vibrational energies than for nonreactive ones, though at higher vibrational energies the shape for both nonreactive and reactive dissociative processes is the same. The main difference between reactive and nonreactive dissociative processes is in general the absolute value of the opacity function. For reactive processes it is nearly twice that of nonreactive ones. This feature is largely amenable to the fact that a larger number of channels leads to reactive dissociation (four) than to the nonreactive one (two).

Another difference between the opacity functions for the nonreactive and reactive dissociative processes shows up when an initial molecule is highly excited while the other has low excitation. In these cases, the opacity function for the nonreactive processes extends to impact parameters larger than those of reactive processes. Such a behavior explains the higher values of k_{n_d} with respect to k_{r_d}.

For both reactive and nonreactive dissociative processes, an increase of the temperature is effective only when vibrational energy is low. In this case, an increase of the temperature leads to an increase of the probability at small impact parameters, and the formation of the plateau begins at lower vibrational energies. On the contrary, the temperature has no effect when vibrational energy is high.

Another interesting effect of increasing the temperature is the diminishing of direct attacks for nonreactive dissociation when one initial molecule has a high vibrational energy (this becomes even more evident when the vibrational energy of the other initial molecule is low). This feature indicates that at both high temperature (as the ones considered here) and high vibrational energy (at least for one of the reactant molecules) less direct collisions are likely to break the two initial bonds.

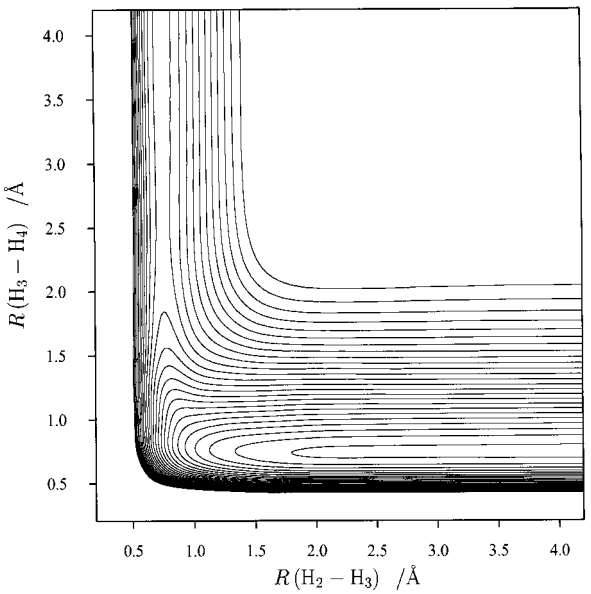

Figure 4. Isoenergetic contours for the collinear $H_1H_2 + H_3H_4$ PES calculated at a fixed value of the H_1H_2 internuclear distance $R(H_1H_2) = 1.41$ Å plotted as a function of the $R(H_2-H_3)$ and $R(H_3-H_4)$ distances. The energy zero is set at the asymptotic equilibrium position in the entrance channel (the lowest contour corresponds to 60 kcal/mol). Energy increments are of 4 kcal/mol.

On the contrary, direct collisions find it difficult to break the initial molecules especially when one of them has a low vibrational energy and cannot act as an energy reservoir. Once both initial bonds are broken, the two atoms can recombine in any order to produce a molecule.

A further comment on the opacity function of the full-dissociative (dashed−dotted lines in Figures 2 and 3) process is deserved. As an example, when $v_{1-2} = v_{3-4} = 13$, at all temperatures, the opacity function shows a plateau ranging from $b = 0$ to $b = 3.5$ Å (with the height of the plateau depending on the temperature) and a subsequent decrease. The width of the plateau decreases as the vibrational numbers decrease and the opacity functions become approximately linear with *b*.

It is worth pointing out that some of the curves plotted in Figures 2 and 3, refer to the aggregated opacity functions from equivalent processes. In particular, the opacity functions of *r* (reactive) processes result from the sum of the two (identical because independent of the labeling of the atoms) opacity functions of processes P1 and P2. The opacity functions for r_d reactive dissociative processes are the sum of the four (again identical because independent of the labeling of the atoms) opacity function for processes P4−P7.

However, the opacity functions for n_d nonreactive dissociative processes are the sum of the two different contributions: the opacity functions for processes P3 and P8. The opacity functions shown in Figures 2 and 3 look like the opacity functions of dissociative processes of molecules having a high vibrational excitation (process P3 when $v_{3-4} > v_{1-2}$ and process P8 when $v_{1-2} > v_{3-4}$). On the contrary, the (much less important) dissociation of molecules having low vibrational excitation leads to smaller values of the opacity function as both the vibrational number and the temperature decrease. They also tend to depend linearly on *b*. This means that the impact parameter plays a different role on the nonreactive dissociation of molecules having high and low vibrational energy.

To better understand the nature of the opacity function, we plotted in Figures 4 and 5 the isoenergetic contour maps of the PES. To mimic the situation occurring for two different values

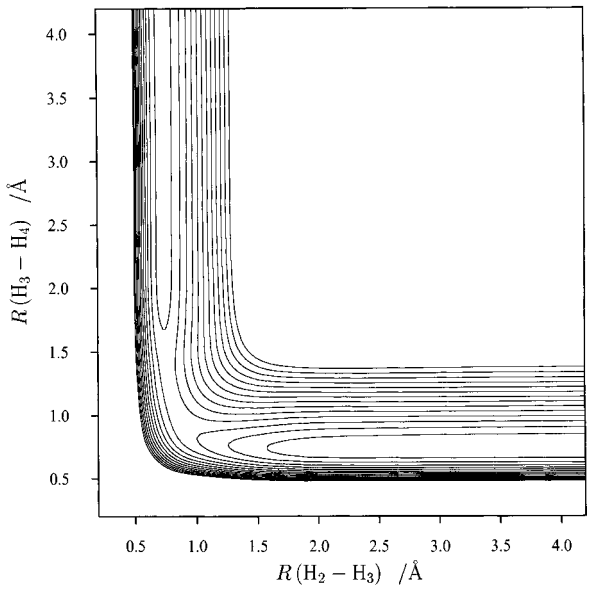

Figure 5. Isoenergetic contours for the collinear $H_1H_2 + H_3H_4$ PES calculated at a fixed value of the H_1H_2 internuclear distance $R(H_1H_2) = 2.16$ Å plotted as a function of the $R(H_2-H_3)$ and $R(H_3-H_4)$ distances. The energy zero is set at the asymptotic equilibrium position in the entrance channel (the lowest contour corresponds to 104 kcal/mol). Energy increments are of 4 kcal/mol.

of the initial vibrational state of the target hydrogen molecule, two different internuclear distances were used. As is shown by the figures, the exchange channel opens when the molecules get closer at high vibrational energy (larger internuclear distance). On the contrary, the potential is strongly repulsive when both molecules have a low vibrational energy. This means that, at zero-impact parameter, molecules in low vibrational states collide as hard spheres, whereas molecules in high vibrational states can easily overcome the barrier to exchange that decreases as the vibrational energy increases. At the same time, an increase of the temperature is able to provide more translational energy useful to overcome the barrier. This favors both reaction and dissociation because the dissociation energy of the H_2 molecule is larger than the exchange barrier.

Vibrational Distributions

Other quantities providing useful clues on the nature of the reactive mechanisms are the product distributions. Product rotational distributions are thermalized and basically conserve the reactants' distributions. On the contrary, product vibrational distributions (PVD) obtained by plotting the calculated rate coefficients as a function of the vibrational state of the products for a given pair of reactants' vibrational states provide more information. The PVDs for the various processes are given in Figures 6 and 7. In Figure 6, PVDs calculated at $T = 4000$ K for nonreactive processes (inelastic (a) and dissociative (b)) are shown using a solid line for the molecule corresponding to the first vibrational number of the pair and a dotted line for the molecule corresponding to the second vibrational number of the pair. In Figure 7, the same quantities calculated at $T = 4000$ K for reactive processes (both non dissociative (a) and dissociative (b)) are shown.

As mentioned before, several trajectories not undergoing the reactive exchange are purely elastic because they end up by having the same pair of vibrational numbers as the reactants. Because the number of elastic trajectories does not tend to zero with b, we take here into account only those leading to the variation of at least one vibrational number.

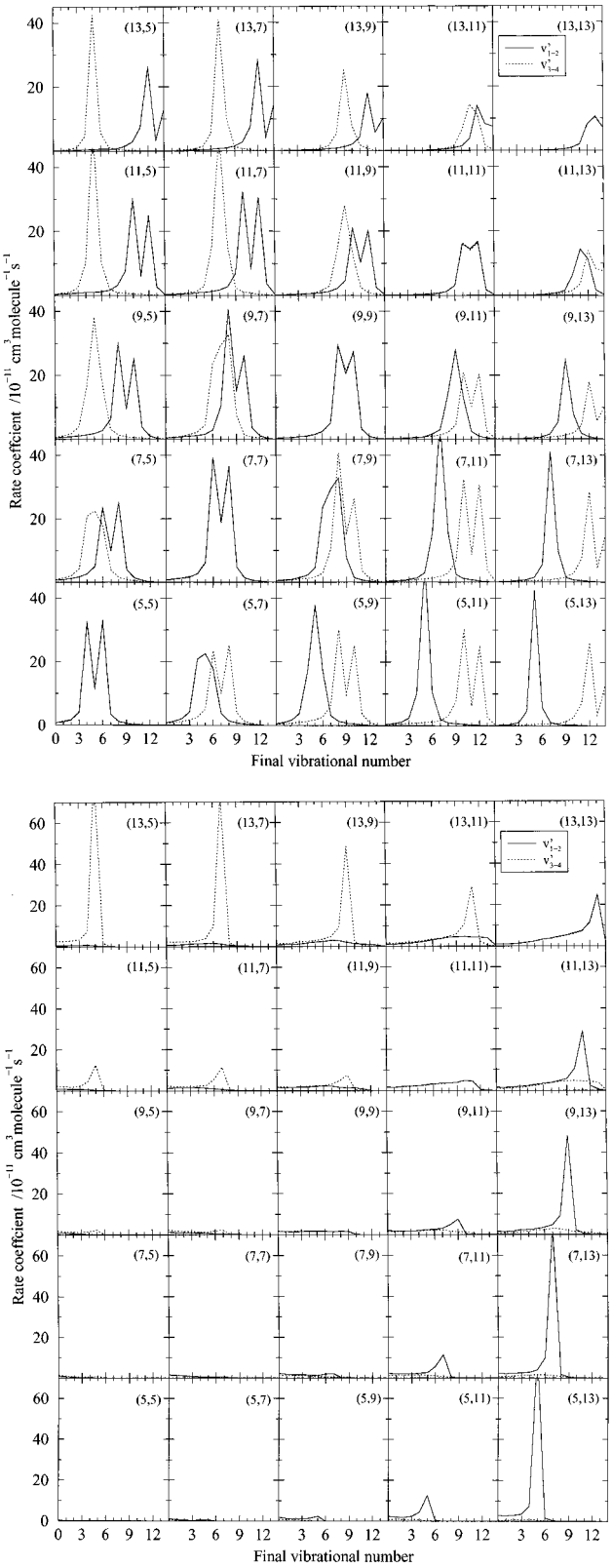

Figure 6. (a) Inelastic rate coefficients calculated at given pairs of vibrational numbers (indicated in brackets) plotted as a function of the final vibrational number for rotationally and translationally thermalized reactants at $T = 4000$ K. Solid and dotted lines are used for the results of the molecule associated with the first and the second vibrational number, respectively. (b) Idem for nonreactive dissociative rate coefficients.

A first interesting feature of the PVD plots is illustrated in Figure 6a. PVDs obtained from both the more and the less vibrationally excited molecule are almost symmetric with respect

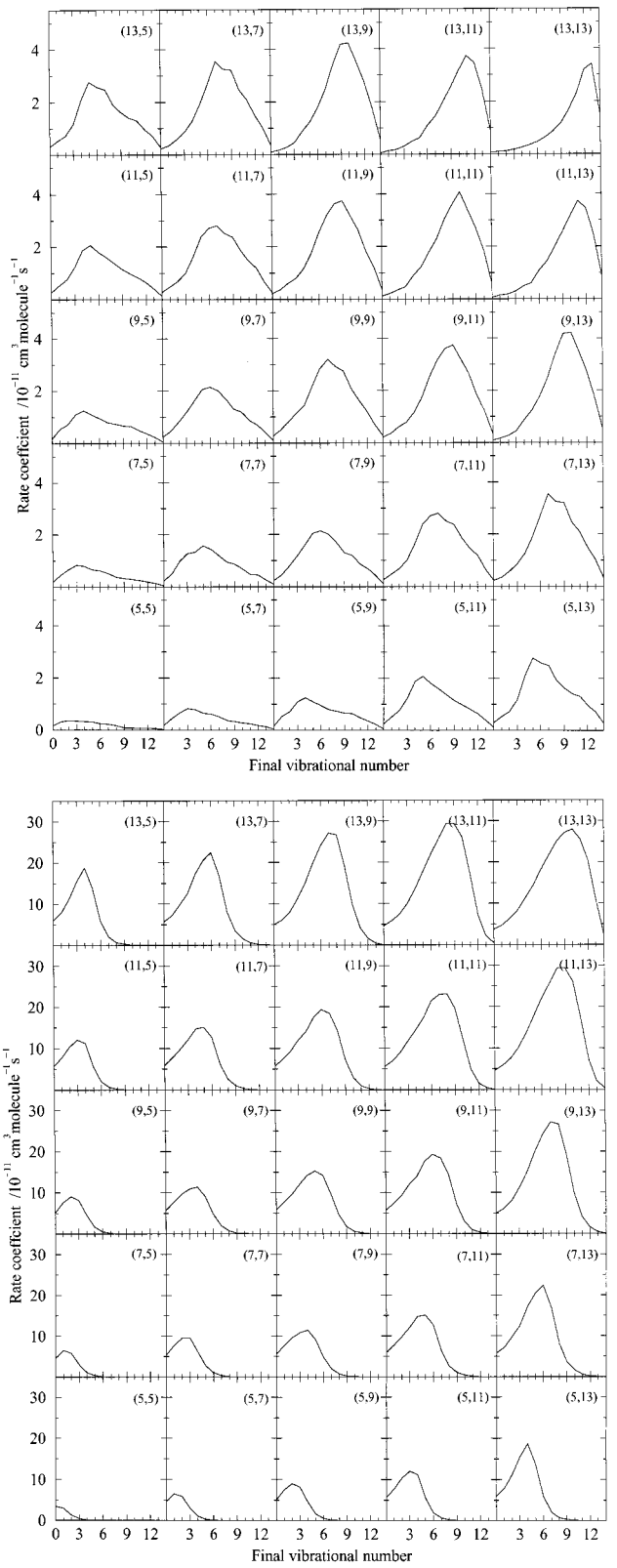

Figure 7. (a) Reactive rate coefficients calculated at given pairs of vibrational numbers (indicated in brackets) plotted as a function of the final vibrational number for rotationally and translationally thermalized reactants at $T = 4000$ K. (b) Idem for reactive dissociative rate coefficients.

to the initial vibrational number. The PVD obtained from the less vibrationally excited molecule peaks at the initial vibrational number, and its height is approximately proportional to the difference between the two initial vibrational numbers. On the contrary, PVDs obtained from the more vibrationally excited molecule have a minimum at the initial vibrational number. This minimum finds its origin in single-molecule inelastic events (whereas the other collision partner does not change its vibrational state). The main difference between the PVDs obtained from the two initial molecules is the width of the distribution: there is a tendency for higher vibrational states to lead to wider distributions, whereas the lower vibrational states get less perturbed during the collision. Obviously, when the two cases coincide, the two curves overlap and the symmetry with respect to the initial vibrational number is preserved.

When dissociation accompanies nonreactive events, as is shown in Figure 6b, the molecule with the highest vibrational number is the most likely to break and to lead to the formation of atomic fragments. A comparison of the upper left-hand side panel with the lower right-hand side panel well illustrates this situation. No matter what the vibrational number is of the intervening molecules, the one remaining not or least unperturbed is always the one having the lowest vibrational excitation. The other molecule involved in the nonreactive collision almost completely dissociates, whereas the final vibrational state is likely to be that of the less-excited molecule regardless of its initial value. This means that the nonreactive dissociative processes are driven by the lowest vibrational state and that even a short interaction time is sufficient to force the more vibrationally excited molecule either to adapt (and lose the excess vibrational energy in favor of that in the lower state) or to not survive (and break up).

The role played by the lowest vibrational level of the reactants is even more evident when the process gets past the transition-state region and an exchange of molecular partners occurs. In Figure 7, values of both aggregated reactive and reactive dissociative rate coefficients are plotted against the final vibrational number. These PVDs are, in general, broad and peak at the lowest level of the reactants or at a nearby (usually lower) level. As a matter of fact, the reactive process starting from $v_{1-2} = 5$ and $v_{3-4} = 7$ shown in Figure 7a has a maximum probability at the product vibrational number 3. Other initial situations, like the $v_{1-2} = 9$ and $v_{3-4} = 7$ or the $v_{1-2} = 9$ and $v_{3-4} = 13$ ones lead to a PVD peaking at 6 and 10, respectively. The most significant exception is the $v_{1-2} = v_{3-4} = 13$ case for which the PVD peaks (though with a minimum difference with 12) at 13. The peculiarity is due to the fact that this state is close to the dissociation continuum.

This is also confirmed by the PVDs shown in Figure 7b for reactive dissociative processes whose permanence in the strong interaction region of the transition state allows to an exchange of the molecular partners (and, in this case, also to dissociation). These PVDs have a similar shape even though with a larger absolute value. It is again worth noticing, here, the strong contribution of exchange on the maximum of the PVD (that is, lower than that of pure reaction) and on its shape that extends to small vibrational energies and drops sharply for high energies.

A change in temperature varies the value of the rate coefficients without modifying the vibrational distribution. This is true for all types of processes. The most remarkable exception occurs for the inelastic PVD associated with the two initial molecules having a similar small vibrational energy. In these cases, the symmetry of the PVD is lost because the two molecules lose their initial vibrational excitation.

Conclusions

Extended QTC calculations were carried out for the $H_2 + H_2$ collision at various values of the initial vibrational quantum

number and at thermalized rotational and translational energies. The calculations showed that for this system inelastic processes dominate at low vibrational energy, whereas dissociation takes the lead when at least one reactant molecule is highly vibrationally excited.

Another important feature found by the calculations is that the exchange of molecular partners (reaction) is very important (despite the high barrier to reaction) even when the process is dissociative. To this end, the lightness of H and the symmetry of the $H_2 + H_2$ system play a key role.

Help to the rationalization of the reaction dynamics is provided by the study of the opacity function. For inelastic processes the shape of the opacity function is very close to that of the hard sphere. However, as the vibrational energy of the reactants increases, the height of the plateau decreases, whereas the interval of the contributing impact parameter values widens in agreement with the increased average value of the internuclear distance of the reactant molecule. A particularly interesting effect was found to take place when increasing the vibrational energy of both reactant molecules. In this case, the opacity function was found to become inverted, with a maximum at fairly large values of the impact parameter. The opacity function for reactive processes shows, on the contrary, a maximum at low impact parameters that rapidly dies off as *b* increases, giving some credit to the assumptions of the RD model.

The calculations show also that only vibrationally excited molecules act as an energy reservoir, and low excited molecules are only slightly perturbed during the collision.

Acknowledgment. Partial financial support from the spanish DGES (PB98-0281), and the Italian MURST, ASI and CNR is acknowledged. This work has been carried out as a part of the COST in Chemistry European Cooperative Project D9/0003/97.

References and Notes

(1) Clary, D. C. *J. Phys. Chem.* **1994**, *98*, 10678. Bowman, J. M.; Schatz, G. C. *Annu. Rev. Phys. Chem.* **1995**, *46*, 169.
(2) Martin, P. G.; Keogh, W. J.; Mandy, M. E. *Astrophys. J.* **1998**, *499* (*2*), 793.
(3) Schwenke, D. W. *J. Chem. Phys.* **1990**, *92*, 7267.
(4) In *Non equilibrium processes in partially ionized gases*; Capitelli, M., Barsdley, J. N., Eds.; Plenum: New York, 1990.
(5) Gorse, C.; Capitelli, M.; Bacal, M.; Bretagne, J.; Laganà, A. *Chem. Phys.* **1989**, *117*, 177.
(6) Bauer, S. H. *Annu. Rev. Phys. Chem.* **1979**, *30*, 271.
(7) Lifshitz, A.; Bidani, M.; Carrol, H. F. *J. Chem. Phys.* **1983**, *79*, 2742.
(8) Rohlfing, E. A.; Rabitz, H.; Gelfand, J.; Miles, R. B.; De Pristo, A. E. *Chem. Phys.* **1980**, *51*, 121.
(9) Rohlfing, E. A.; Gelfand, J.; Miles, R. B.; Rabitz, H. J. *J. Chem. Phys.* **1981**, *75*, 4893.
(10) Rohlfing, E. A.; Rabitz, H.; Gelfand, J.; Miles, R. B. *J. Chem. Phys.* **1984**, *81*, 820.
(11) Kreutz, T. G.; Gelfand, J.; Miles, R. B.; Rabitz, H. J. *Chem. Phys.* **1988**, *124*, 359.
(12) Arnold, J.; Dreier, T.; Chandler, D. W. *Chem. Phys.* **1989**, *133*, 123.
(13) Hernandez, M. I.; Clary, D. C. *J. Chem. Phys.* **1996**, *104*, 8413.
(14) Ceballos, A.; Garcia, E.; Rodriguez, A.; Laganà, A. *Chem. Phys. Lett.* **1999**, *305*, 276.
(15) Cacciatore, M.; Billing, G. D. *J. Phys. Chem.* **1992**, *96*, 217 and references therein.
(16) Mandy, M. E.; Martin, P. G.; Keogh, W. J. *J. Chem. Phys.* **1998**, *108*, 492.
(17) Keogh, W. J. Ph.D. Thesis, University of Toronto, Toronto, Canada, 1992.
(18) Aguado, A.; Suarez, C.; Paniagua, M. *J. Chem. Phys.* **1994**, *101*, 4004. We thank the authors for supplying us with a fortran routine of the potential.
(19) Boothroyd, A. I.; Dove, J. E.; Keogh, W. J.; Martin, P. G.; Peterson, M. R. *J. Chem. Phys.* **1992**, *95*, 4331.
(20) Hase, W. H.; Duchovic, R. J.; Hu, X.; Komornicki, A.; Lim, K. F.; Lu, D.; Peslherbe, G. H.; Swamy, K. N.; Vande Linde, S. R.; Varandas, A.; Wang, H.; Wolf, R. J. *VENUS96: A General Chemical Dynamics Program*, QCPE Program, N. 671; Indiana University: Bloomington, Indiana.
(21) Truhlar, D. G.; Muckerman, J. T. In *Atom−Molecule Collision Theory*; Bernstein, R. B., Ed.; Plenum: New York, 1979; p 505.